The detection and quantification of food components on stainless steel surfaces following use in an operational bakery

Whitehead, K. A.*, Saubade, F., Akhidime, I. D., Liauw, C. M., Benson, P. S. and Verran, J.

Microbiology at Interfaces Group, Manchester Metropolitan University, Chester St, Manchester M1 5GD UK

* Tel: 0161 247 1157

E-mail address: K.A.Whitehead@mmu.ac.uk

Abstract

Food preparation areas in commercial bakeries present surfaces for continual organic fouling. The detection of retained food components and microorganisms on stainless steel surfaces situated for one month in the weighing in area, pastry and confectionary production areas of a bakery were investigated using different methods. Scanning electron microscopy demonstrated the morphology of the material on the surfaces from all three areas, with the weighing in area demonstrating a more even coverage of material. Differential staining assays demonstrated a high percentage coverage of organic material heterogeneously distributed across the surfaces. Differential staining also demonstrated that the amount of organic material on the surface from the confectionary area was significantly greater than from both the pastry and weighing in areas. Although, UV at 353 nm did not detect residual surface fouling, performance of the UV detection was optimised and demonstrated that the residual organic material on the weighing in area and the pastry samples was best illuminated at 510 - 560 nm, and from the confectionary area of the bakery at 590 - 650 nm. ATP bioluminescence revealed the confectionary production area contained the highest level of biofouling. Contact plates determined that only low microbial counts ($\leq$ 2) CFU/cm^2) were recovered from the surfaces. Changes in the physicochemistry (increased hydrophobicity) demonstrated that all the surfaces were fouled (ΔG_{iwi} -26.8 mJ/m^2 to -45.4 mJ/m^2). Fourier Transform Infra-Red Spectroscopy (FTIR) demonstrated that all the surfaces had retained fats,

carbohydrates and proteins. This work suggests that a range of methods may be needed to fully detect organic and microbial fouling.

Keywords: Biofouling; food; conditioning film; detection; bakery; microorganisms

1. Introduction

Operational efficiency in food processing industries is affected by the fouling of preparation surfaces, which is often due to the raw food materials. Fouling of food contact surfaces occurs as a result of the transfer or buildup of adsorbed organic material on food processing surfaces. If such fouling becomes problematic, it may impact the overall product quality and increase the operational costs of food production due to frequent shut downs for cleaning (Barish and Goddard, 2013). Biofouling leads to the production of a conditioning film on the food preparation surface, which can influence subsequent microbial attachment and/or biofilm formation (Whitehead et al. 2008; Whitehead et al. 2010).

In commercial bakeries, the ingredients include flour, yeast, salt, water, and oil/fat (Chen et al. 2005), which are all ideal for the formation of organic conditioning films on the surfaces. In addition, they are a good source of nutrients for microorganisms. Therefore, food preparation surfaces in bakeries present an interface for continual soiling as the food ingredients used in production process are high in organic matter content, which easily disperse to form films on the surfaces. It has been reported that the organic material involved in the fouling of surfaces influences substratum properties and cell attachment and microbial retention with a subsequent impact on the microbial fouling of surfaces (Whitehead et al. 2008).

Stainless steel is one of the most common materials used in bakery equipment (Chen et al. 2005). The retention of organic material on industrial surfaces leads to such surfaces becoming a potential nutrient source for microbial growth. These surfaces will then be new sources of microorganisms transfer, which can lead to food contamination (Whitehead et al. 2010). Bacterial contamination of food processing equipment is a central concern owing to the potential food spoilage and transmission of foodborne pathogens.

There are currently a range of detection methods (e.g. Adenosine Triphosphate (ATP) bioluminescence and Ultra Violet (UV)) for use in industry that allow rapid identification of surface fouling. However, previous works have demonstrated that different methods have varying range in

56 the limit of detection for different types of organic fouling (Whitehead et al. 2008; 2009a; 2010;
57 2011). Some of these methods might be optimized, for example, using UV detection the wavelength
58 can be optimised to detect residual organic material present on the surface (Adhikari and Tappel,
59 1975; Whitehead et al., 2010). Optimization of such methods is dependent on the molecular
60 configuration of organic material allows some organic residues to fluoresce Another drawback of
61 these methods is that they do not discriminate between the amount of organic fouling and microbial
62 load (Everard et al. 2016: Salo et al. 2008; Verran and Whitehead 2006).
63 Scanning electron microscopy (SEM) has been utilized for a number of years to visualize both
64 organic material and cells retained on surfaces (Rajab et al. 2018; Whitehead et al. 2005; Zouaghi
65 et al. 2018) as has differential staining methods (Whitehead et al. 2009b). Fourier Transform Infra-
66 Red Spectroscopy (FTIR) has been used to detect the fouling retained on surfaces (Whitehead et
67 al. 2011), however it can also be used to detect bacteria retained on surfaces (Schmitt and
68 Flemming, 1998). Although these and other methods have been carried out to detect organic fouling
69 and microbial contamination *in vitro,* to the authors knowledge, a comparison of such detection
70 methods have not been used to determine the amount of residual biofouling on surfaces from a
71 working bakery.
72 The aim of this work was to compare the detection and quantification of organic fouling on surfaces
73 recovered from a bakery following one month exposure.

74 **2. Methods**

75 A range of methods were used to determine and compare the detection of residual fouling and
76 microorganisms on stainless steel surfaces following their *in situ* placement for one month in a
77 working bakery which produced a variety of confectionaries.

78 *2.1 Sampling site and sample substrata*

79 A bakery in the Northwest of England, UK, served as a host site where samples of stainless steel
80 plates were placed on site prior to surface analysis investigations. The bakery used in this work
81 produced both confectionary and pastry products. Stainless steel plates (2 mm thick, 340 2B finish)

were cut using an industrial hydraulic guillotine into 200 mm x 200 mm sample pieces and placed in the bakery for one month. The stainless steel sample pieces were placed in three areas of the industrial bakery; the weighing in area (where bags and boxes of food material are brought into the bakery and dispensed), the pastry preparation area and the confectionary production area. The stainless steel surfaces were exposed to the same routine food production and cleaning processes as other work surfaces in the bakery. In the bakery's cleaning regime, workbenches surfaces were cleaned each evening using a wipe method with the sanitizer Aphemclen® following the manufacturer's instructions (Selden, UK). Following the *in situ* placement, samples were cut into smaller substrata (20 x 20 mm) and used for subsequent surface analysis.

2.2 Determination of surface fouling.

2.2.1 ATP Bioluminescence

ATP bioluminescent measurements were carried out using an ATP bioluminescent device (Hygiena, UK), operated as per the manufacturer's instructions. However, although the manufacturer recommended swabbing a 100 x 100 mm area, in this study, both a 40 x 40 mm and 100 x 100 mm surface area were swabbed and the results were compared. Results were classified according to the manufacturers guidance whereby a result of < 10 relative light units (RLU) means that the surface could be considered clean, ≥ 10 to ≤ 29 RLU indicated that the surface was not adequately clean and >30 RLU the surface required cleaning (n = 3).

2.2.2 UV detection

A UV lamp (Labino trac-pack) with a lamp range of 353 nm was used for UV analysis of substrate surface. The optimum wavelengths of UV to illuminate the different soils were then determined by visualizing soil samples with different filters (330 nm - 380 nm, 510 nm - 560 nm and 590 nm - 650 nm) using an Epifluorescence microscope (Nikon Eclipse E600, UK). For all UV illumination, the unstained samples were place under the UV and the qualitative detection of biofouling on the sample was recorded (n = 5).

2.2.3 Epifluorescence microscopy

The substrata were visualized using Epifluorescence microscopy (Nikon Eclipse E600, UK) with an F-View II black and white digital camera (Soft Imaging System Ltd, UK) using a Cell F Image Analysis package (Olympus, UK). The percentage coverage area of the stained material was measured to indicate the surface coverage of the organic material (n = 60).

2.2.4 Scanning electron microscopy (SEM)

Samples of the stainless steel surfaces for observation by SEM were prepared. The surfaces were immersed in 4 % v/v gluteraldehyde (Agar Scientific, UK) for 24 h at 4 °C, washed in sterile distilled water, dried and stored at room temperature, in phosphorous pentoxide (Sigma Aldrich, UK) desiccators. The samples were sputter coated at a vacuum of 0.0921 mbar, for 3 min, at 2500 V, in argon gas at a power of 18-20 mA (Polaron E5100 SEM sputter coater, UK). Images of the control and fouled substrata were obtained (JEOL JSM 5600LV Scanning electron microscope, UK) (n = 3).

2.2.5 Fourier transform infrared spectroscopy

The stainless steel coupons (n=5) were analysed in reflection mode using a Nicolet Continuum FTIR microscope (with liquid nitrogen cooled MCT detector) fitted to a Nicolet Nexus FTIR bench. The apertures were set to maximum opening, 200 µm x 200 µm. Spectra were made up of 120 scans with resolution set to 4 cm^{-1}. All spectra were converted to absorbance and baseline corrected using a spline fit. As the sampling area was fixed at 200 µm x 200 µm, it was possible to use the combined areas ($A_{(combined)}$) of the OH and CH stretching ($A_{(OH\&CH)}$), carbonyl (including amide) ($A_{(C=O)}$) and C-O stretching peaks ($A_{(C-O)}$) as a measure of the relative amount of organic matter, as summarized by equation 1.

$$A_{(combined)} = A_{(OH\&CH)} + A_{(C=O)} + A_{(C-O)} \quad (1)$$

Peak areas were determined using the integration tool within the Nicolet Omnic software. The integration limits varied from spectrum to spectrum due to differing peak width, though

approximate integration limits were as follows: $A_{(OH\&CH)}$ 3710 – 2500 cm^{-1}; $A_{(C=O)}$ 1780 – 1490 cm^{-1} and $A_{(C-O)}$ 1780 – 760 cm^{-1}s. The baseline limits were the same as the integration limits. The averages of five replicate $A_{(combined)}$ values were reported together with the standard deviation and the percentage ratio of the standard deviation to the average value.

2.2.6 Differential staining of organic material and microorganisms

Differential staining of the sample surfaces was carried out. Ten microliters of 4', 6-diamidino-2-phenylindole dye (DAPI, UK) was applied to the surface and spread across the sample surface using a sterile plastic spreader, followed by the addition and spread of 10 µL of rhodamine (Sigma, UK). The samples were incubated for 10 min and then thoroughly rinsed with distilled water and dried in a class 2 laminar flow hood in the dark for 1 h. The samples were visualized and analysed using an epifluorescent microscope (Nikon Eclipse E600, UK).

2.2.6 Contact plates

The contact plate method for evaluating viable microbial counts from the surface of the substrata was adapted from Eginton et al. (1995). The method involved using Plate Count Agar (PCA), de Man, Rogosa, Sharpe agar ((MRS), for *Lactobacillus* detection), Tryptone soya agar (TSA), Brain heart infusion agar (BHIA), Sabouraud agar ((SAB), for detection of moulds and yeast) and MacConkey agar (for detection of *Escherichia coli*) all prepared according to the manufacturer's instructions (Oxoid, UK). Stainless steel plates (20 mm x 20 mm) were placed onto the agar for 1 min, then removed. The agar was incubated for 24 h – 48 h at 30°C to allow the bacterial and fungal cultures to grow. The microorganisms recovered from the plates were isolated onto the appropriate agars to obtain pure cultures (n = 3).

Physicochemistry of surfaces

The physicochemistry of the surfaces was characterized according to Wilson-Nieuwenhuis et al. (2017). Contact angles (θ) using HPLC grade water (BDH, UK), ethylene glycol or dioodomethane (Alfa Aesar, USA) were measured with a MobileDrop goniometer (Krüss GMBH, Germany). Both advancing and receding angles were determined, with five

measurements of each chemical on each sample taken (n = 10). Fresh coupons were used for each solvent to ensure there was no cross contamination of solvents on the surfaces. The methods of van Oss et al. (1988) and van Oss and Giese (1995) was used for calculating the surface energy (γ_s^{SE}) of the films from these measurements, according to the following equation:

$$(1 + \gamma_l)\, cos\theta = 2\left(\sqrt{\gamma_s^{LW}\gamma_l^{LW}} + \sqrt{\gamma_s^{A}\gamma_l^{B}} + \sqrt{\gamma_s^{B}\gamma_l^{A}}\right) \quad (2)$$

where the subscripts *s* and *l* denote the surface energy of the solid and liquid respectively. The superscript *LW* denotes the Lifshitz-van der Waals components of the surface energy, and the superscripts *A* and *B* denote the Lewis acid and Lewis base parameters of the surface energy. The acid and base terms can be combined into the Lewis acid base (superscript *AB*) component of the surface energy:

$$\gamma_i^{AB} = 2\sqrt{\gamma_i^{A}\gamma_i^{B}} \quad (3)$$

Subsequently the overall surface energy was calculated as the sum of the Lifshitz-van der Waals and Lewis acid base components:

$$\gamma_i = \gamma_i^{LW} + \gamma_i^{AB} \quad (4)$$

The components of the surface energy were then used to assess the hydrophobicity, or Gibbs free energy of attraction between the surface and liquid (surface energies are denoted by subscript *w*), and were calculated using the following[22]:

$$\Delta G_{sw} = -2\left(\left(\sqrt{\gamma_s^{LW}} - \sqrt{\gamma_l^{LW}}\right)^2 + 2\left(\sqrt{\gamma_s^{a}\gamma_s^{b}} + \sqrt{\gamma_l^{a}\gamma_l^{b}} - \sqrt{\gamma_s^{a}\gamma_l^{b}} - \sqrt{\gamma_l^{a}\gamma_s^{b}}\right)\right) \quad (5)$$

2.2.7 Statistical analysis

The results were averaged and the standard deviation of the results calculated, and applied as error bars. T-tests were carried out to determine the significant variance in the data whereby $p < 0.05$ was considered significant.

3. Results

The ATP bioluminescence investigation revealed the presence of ATP on all the surfaces in all the areas analyzed (Figure 1). There were no significant differences determined between the amount of organic material demonstrated on the control and the weighing in area (40 mm x 40 mm control = 5 RLU, weighing in area = 3.6 RLU; 100mm x 100 mm control = 7.7 RLU, weighing in area = 2.6 RLU). This suggests that both the control surfaces and the coupons deposited for one month in the weighing in area can be considered as clean. The stainless steel samples from the pastry area and confectionary area were significantly different. The pastry area demonstrated that the surfaces were adequately clean (40 mm x 40 mm 13.3 RLU, 100mm x 100 mm = 13 RLU), whilst the confectionary area demonstrated the greatest amount of fouling (40 mm x 40 mm = 57.3 RLU, 100mm x 100 mm = 59 RLU). The confectionary area demonstrated RLU levels 15 times that of the weighing in area and 4 times that of the pastry indicating a highest organic matter presence. Regardless of the area size, there was no significant difference between the bioluminescence results of the 40 mm x 40 mm and the 100 mm x 100 mm areas investigated.

The investigations using the UV illumination carried out with the standard lamp at 353 nm revealed no differences observed between the control surfaces and the surfaces recovered from the three areas of the bakery (Figure 2a-d).

In order to optimize the UV illumination, the surfaces were exposed to different wavelengths of UV, so that the residual organic material on the surfaces were illuminated. The results demonstrated that residual organic material on the surfaces from the weighing in area and the pastry area were best illuminated by UV in the 510 - 560 nm.For the confectionary area of the bakery the best results were achieved in the 590 - 650 nm (Figure 3). And so? Do we have a percentage coverage to say which surfaces were the most fouled, according to this detection method?

209 Scanning Electron Microscopy (SEM) was used to visualise the residual materials on the surfaces.
210 SEM results demonstrated that the control surfaces were clean (Figure 4a), whereas the surfaces
211 recovered from the weighing in area looked to have organic material distributed across the surface
212 (Figure 4b). Images from the pastry and confectionary areas demonstrated the presence of
213 particulate fouling (Figures 4 c and d). These results indicate that fouling occurred on the surfaces
214 in the three areas of the bakery.
215 Following the differential staining assays, it was revealed that organic material was
216 heterogeneously dispersed across all surfaces used in the investigation (Figures 5b-d), when
217 compared to the control (Figure 5a). Indeed, samples taken from all areas of the bakery indicated
218 presence of organic material in the grain boundaries (Figures 5b-d). However, the surfaces from
219 the pastry area showed the greatest amount of coverage (71.0 %) when compared to the weighing
220 in area (65.2 %) and confectionary areas (59.0 %) (Figure 5e). The organic material on surfaces
221 from the confectionary area was significantly different ($p < 0.05$) from both the pastry and
222 weighing in areas.
223 Following the contact plate assays onto the different types of agar, low numbers of bacteria, yeasts
224 and moulds were isolated from the surfaces tested (< 2 CFU/cm^2) (Figure 6). No *Lactobacillus* or
225 *Escherichia coli* were detected from any of the samples taken from the bakery on the MRSA or
226 MAC agar contact plates respectively.
227 The physicochemical results demonstrated that, following use in the bakery, all the surfaces became
228 more hydrophobic ($\Delta Giwi$ comprised between -26.8 mJ/m^2 and -45.4 mJ/m^2) compared to the
229 control ($\Delta Giwi$ = -18.0 mJ/m^2) (Table 1). The γs^+ decreased from 0.55 mJ/m^2 for the control
230 surfaces, to 0.2 mJ/m^2 for the other surfaces. The γs^{LW} values slightly increased from 34.4 mJ/m^2
231 on the control surfaces to 35.6 mJ/m^2– 39.4 mJ/m^2 on the used bakery surfaces. The γs^{AB} values
232 decreased from 6.2 mJ/m^2 on the control surfaces to 2.3-3.1 mJ/m^2, as did the γs^- values from 17.4
233 mJ/m^2 on the control surfaces to 8.2 mJ/m^2 – 14.4 mJ/m^2 on all the surfaces recovered from the
234 bakery.

Surface contamination was assessed using FTIR. Representative spectra from each of the three sampling areas from within the bakery are shown in Figure 7. Surfaces from all three areas of the bakery demonstrated significant common peaks that can be summarized as follows:

i) hydrogen bonded N-H and O-H stretching (3700 cm^{-1} – 2600 cm^{-1}) from adventitious water, sugars/carbohydrates (from flour) (O-H) and proteins (N-H),

ii) C-H stretching vibrations (3000 cm^{-1}– 2800 cm^{-1}) mainly due to fatty alkyl chains

iii) Carbonyl stretching (1780 cm^{-1} – 1490 cm^{-1}) due to fatty esters and amide groups of proteins,

iv) C-O bending 1170 cm^{-1} – 800 cm^{-1}, due to ether linkages in sugars / carbohydrates and esters in fats.

The absorption bands in the spectra obtained from the confectionary area indicated that there was contamination, potentially from flour (C-O correlation), sugar (C-O correlation) and fat (ester carbonyl correlation). There were also some proteins, indicated by amide I and II bands, present in all the samples, which could be due to gelatin (setting agent) residues. The pastry area showed contamination with diverse mixtures of fats and proteins. The weighing in area also showed a diversity of contaminants with thick fat and flour contamination. The average combined OH/NH stretch, carbonyl, protein amide and C-O stretching peak areas ($\overline{A_{(combined)}}$) from the FTIR spectra together with the standard deviation values for the data provide insight into the differences in levels and uniformity of contamination within a particular area of the bakery (Table 2). The weighing in area showed by far the highest level of fouling and also showed the most non-uniform fouling, as indicated by the very high SD relative to the average value. The pastry and confectionary areas had substantially lower levels of fouling; combined peak area values were broadly similar and the SD values relative to the average indicated greater uniformity of fouling compared with the weighing area.

4. Discussion

Biofouling of industrial surfaces is of a major concern. When a food product comes into contact

261 with a stainless steel work surface, the contact surface will become contaminated with organic
262 material, and potentially microorganisms (Whitehead et al. 2011). Cleaning procedures aim to
263 remove organic material and microorganisms, but there is concern regarding organic material and
264 microorganisms that are retained on surfaces. There are numerous ways to detect organic and
265 microbial fouling on a surface. However, there is little information comparing the methods on
266 surfaces taken from a food industry. As a result, it is difficult to choose the best method to assess
267 the cleanliness of a surface in a food industry. In this study, the detection of both organic material
268 and microorganisms using different detection/quantification methods has been assessed on surfaces
269 recovered from a bakery, following one month exposure.
270 ATP bioluminescence has been widely used for the detection of microbial contamination and food
271 residues in the food industry (Everard et al. 2016), providing a real time estimate of total surface
272 cleanliness, including the presence of organic debris and microbial contamination. In this work, the
273 ATP reading in the confectionary area was five times greater than that of the pastry area. It may be
274 that on the confectionary surface, since sugar is water soluble and is easy to remove, oils are
275 difficult to remove, and protein is very difficult to remove (Corrieu et al. 1981), that ATP was
276 recovered from the surfaces with the most soluble organic component.
277 The use of UV has been shown to be a reliable, quick and cost effective method of accessing
278 hygiene after cleaning processes in both closed (Salo et al. 2008) and open surfaces (Verran and
279 Whitehead 2006). The need for rapid industrial detection methods such as UV is important in
280 determining the efficiency of cleaning and disinfection against organic soil and cell retention. UV
281 (353 nm) can be used for the detection of residual cells and soiling on industrial surfaces, although
282 (as with ATP) no distinction is made between the two components (Whitehead et al. 2009b). Using
283 the regular 353 nm UV lamp, the level of contamination was too low on the surfaces recovered
284 from the bakery to demonstrate residual fouling. However, using the UV with different wavelength
285 filters, it was demonstrated that the residual organic material were best illuminated in the 510 - 560
286 nm for the weighing in area and pastry areas, and in the 590 - 650 nm for the weighing in areas.

This occurs because the molecular configuration of organic material allows some organic residues to fluoresce when illuminated by UV (Adhikari and Tappel, 1975). This is in agreement with work carried out previously, whereby surfaces with residual fats were best illuminated using this method (Whitehead et al. 2008). This result also corresponds to the surfaces in this work becoming more hydrophobic, and non-polar as demonstrated from the physicochemistry assays. Furthermore, in agreement with our work, Abban et al. (2014) demonstrated that one can change filters on the lamp so that alternative wavelengths suitable for the various material surfaces are used to ensure that residues on different material surfaces could be better visualized and thus the confidence in the validation of the surface hygiene is increased.

SEM has been utilized for a number of years for the visualisation of cell:substratum interactions (Rajab et al. 2018; Whitehead et al. 2005; Zouaghi et al. 2018). It was demonstrated that the control surfaces were clean, whereas the surfaces recovered from the weighing in area looked to have organic material distributed across the surface. Images from the pastry and confectionary areas demonstrated the presence of particulate fouling, which is more reminiscent of protein and carbohydrate fouling (Whitehead et al. 2010). However, the weighing in area demonstrated a surface coverage which was more similar to the residual material left by fat deposits. This corroborates with the results from the weighing in area surfaces, which was demonstrated to have increased γ_S^{LW} measurements, and a more hydrophobic surface.

The development of novel staining systems has allowed quantitative and separate measurement of cells and food soils retained on surfaces (Whitehead et al. 2009b). The differential staining results demonstrated that the organic material was heterogeneously dispersed across all the surfaces used in the investigation, and that it was particularly evident in the grain boundaries of the stainless steel. Additionally, bacteria were not detected which correlates with the microbial counts obtained.. However, this could be because the areas analysed were much smaller than those covered using the contact plate method. The pastry area showed the greatest amount of coverage when compared to the weighing in area and confectionary areas.

313 The microbial investigation of the surfaces revealed an extremely low presence of microbial
314 contamination on the surfaces incubated in the bakery. The microbial data from the contact plates
315 was corroborated by the differential staining and SEM results, both of which indicated no incidence
316 of bacteria on the surfaces. This suggests that although organic material was retained on the
317 surfaces, this did not enhance microbial retention. The number of bacteria detected using the
318 manual counts was not detected using the differential stain, but this could be because the contact
319 plates used a much larger area than the differential staining method. Thus, the level and type or
320 organic material deposited on a surface and its effect on microbial retention merits further
321 investigation.
322 The physicochemical results demonstrated that following use in the bakery, all the surfaces became
323 more hydrophobic compared to the control with increased γs^+ and γs^{LW} values. The γs^{AB} values
324 decreased as did the γs^- values on all the surfaces recovered from the bakery. This suggests that
325 following use, the surfaces became more electron accepting, and apolar. Previous work has
326 demonstrated that when compared to a pristine surface, *in situ* increases or decreases in the surface
327 parameters γs^{AB}, γs^+ (the electron acceptor), and γs^- (the electron donor) suggest the presence of
328 retained surface soil. In agreement with these results changes in $\Delta Giwi$ and γs^{LW} suggest the
329 presence of certain oils and fats retained on the surface (Whitehead et al. 2009a) and this was
330 supported by the FTIR results. Further, Zouaghi et al. (2018) demonstrated that a lower surface
331 energy was shown to be an asset against whey protein deposits on stainless steel surfaces.
332 FTIR can be used to identify molecular species on a surface. FTIR has been used to detect milk
333 traces in food (Cristina et al. 2016) and determine the impact of food treatments on the re-
334 conformation of allergens (Gomaa and Boyce, 2105). The FTIR spectroscopy of the sample areas
335 revealed non-uniform contamination. Quantification of the amount of organic material on the
336 surfaces, using the $\overline{A_{(combined)}}$ values (Table 2), revealed a different ranking of contamination level
337 to the organic coverage and ATP measurements. The weighing area had the highest $\overline{A_{(combined)}}$

338 value, and hence showed the most prolific contamination. This result correlated with the
339 physicochemistry (ΔG_{iwi} value) result and the SEM images.

340 **Conclusions**

341 The different microscopic investigations demonstrated particulate material on the surfaces from all
342 three areas. UV detection was optimised and ATP bioluminescence revealed the confectionary
343 production area contained the highest level of biofouling. Contact plates determined low microbial
344 counts and demonstrated the advantages of screening larger surface areas for microbial
345 contamination. All the fouled surfaces increased in hydrophobicity, which corresponded with the
346 UV and FTIR results. This work suggests that a range of methods may be needed to detect organic
347 and microbial fouling.

348 **Acknowledgements**

349 The research performed has been part of the project FOOD-CT-2005-007081 (PathogenCombat)
350 supported by the European Commission through the Sixth Framework Programme for Research
351 and Development.

352

References

Abban, S., Jakobsen, M., Jespersen, L., 2014. Assessment of interplay between UV wavelengths, material surfaces and food residues in open surface hygiene validation. J. Food Sci. Tech.-Mysore 51, 3977-3983.

Adhikari, H., Tappel, A., 1975. Fluorescent probes from irradiated amino acids and proteins. Radiation Res. 61, 177–183.

Barish, J.A., Goddard, J.M., 2013. Anti-fouling surface modified stainless steel for food processing. Food Bioproducts Processing 91, 352-361.

Chen, Y., Wang, Y., Ge, Y.Q., Xu, B.L., 2005. Degradation of endogenous and exogenous genes of roundup-ready soybean during food processing. J. Agri. Food Chem. 53, 10239-10243.

Corrieu, G., Lalande, M., Roussel, C., 1981. Simplified method to calculate the optimum energy recovery on a plate type milk pasteurizer. Lait 61, 233-249.

Cristina, L., Elena, A., Davide, C., Marzia, G., Lucia, D., Cristiano, G., Marco, A., Carlo, R., Cavallarin, L., Gabriella, G.M., 2016. Validation of a mass spectrometry-based method for milk traces detection in baked food. Food Chem. 199, 119-127.

Everard, C.D., Kim, M.S., Lee, H., 2016. Assessment of a handheld fluorescence imaging device as an aid for detection of food residues on processing surfaces. Food Con. 59, 243-249.

Gomaa, A., Boye, J., 2015. Impact of irradiation and thermal processing on the immunochemical detection of milk and egg allergens in foods. Food Res. Inter. 74, 275-283.

Jullien C, Benezech C, Gentil CL, Boulange-Petermann L, Dubois PE, Tissier JP, Traisnel M, Faille C. 2008. Physico-chemical and hygienic property modifications of stainless steel surfaces induced by conditioning with food and detergent. Biofouling 24:163–172.

Rajab, F.H., Liauw, C.M., Benson, P.S., Li, L., Whitehead, K.A., 2018. Picosecond laser treatment production of hierarchical structured stainless steel to reduce bacterial fouling. Food Bioproducts Processing 109, 29-40.

Salo, S., Friss, A., Wirtanen, G. 2008. Cleaning validation of fermentation tanks. Food Bioproducts Process 86, 204–210.

Schmitt, J., Flemming. H-C. 1998. FTIR-spectroscopy in microbial and material analysis. Inter. Biodeter. Biodeg. 41, 1-11.

Van Oss, C.J., Chaudhury, M.K. Good, R.J. 1988. Interfacial Lifshitz van der Waals and polar interactions in macroscopic systems. Chem. Rev. 88, 27–941.

Van Oss, C.J., Giese, R.F. 1995. The hydrophilicity and hydrophobicity of clay minerals. Clays Clay Miner. 43, 474–477.

Verran, J., Whitehead, K. A. 2006. Assessment of organic material and microbial components on hygienic surfaces. Food and Bioproducts Processing 84 260-264.

Whitehead, K. A., Colligon, J. and Verran, J. 2005. Retention of microbial cells in substratum surface features of micrometer and sub-micrometer dimensions. Colloids Surf. B: Biointerfaces 41, 129-138.

Whitehead, K.A., Smith L. A., Verran J. 2008. The detection of food soils and cells on stainless steel using industrial methods: UV illumination and ATP bioluminescence. Inter. J. Food Microbiol. 127, 121-128.

Whitehead, K. A, Benson, P. Smith, L. A., Verran, J. 2009a. The use of physicochemical methods to detect organic food soils on stainless steel surfaces. Biofouling 25, 749-756.

Whitehead, K. A, Benson, P. Verran, J. 2009b. Differential fluorescent staining of *Listeria monocytogenes* and a whey food soil for quantitative analysis of surface hygiene. Inter. J. Food Microbiol. 135, 75-80.

Whitehead, K.A., Smith L. A., Verran, J. 2010. The detection and influence of food soils on microorganisms on stainless steel using scanning electron microscopy and epifluorescence microscopy. Inter. J. Food Microbiol. 141, S125-S133.

Whitehead, K. A., Benson, P. S., Verran J. 2011. The detection of food soils on stainless steel using Energy Dispersive X-ray and Fourier Transform Infrared Spectroscopy. Biofouling, 27 907-917.

Wilson-Nieuwenhuis, J.S.T., Dempsey-Hibbert, N., Liauw, C.M., Whitehead K.A. 2017. Surface modification of platelet concentrate bags to reduce biofilm formation and transfusion sepsis. Coll. Surf. B: Biointerfaces. 160, 126–135.

Zouaghi, S., Six, T., Nuns, N., Simon, P., Bellayer, S., Moradi, S., Hatzikiriakos, S.G., Andre, C., Delaplace, G., Jimenez, M., 2018. Influence of stainless steel surface properties on whey protein fouling under industrial processing conditions. J. Food Eng. 228, 38-49.

434 Table 1. Physicochemistry (mJ/m^2) results of the surfaces following removal from the bakery site.

	$\Delta Giwi$	γs^{LW}	γs^{AB}	γs^{+}	γs^{-}
Control	-18.0	34.4	6.2	0.5	17.4
Weighing in area	-45.4	38.2	2.3	0.2	8.2
Pastry	-26.8	35.6	2.9	0.2	14.4
Confectionary	-36.3	39.4	3.1	0.2	11.3

435

436

437 Table 2. Average combined OH/NH stretch, carbonyl, protein amide and C-O stretching

438 absorbance peak areas ($\overline{A_{(combined)}}$) and respective standard deviation and SD as % on the

439 average values (n=5 unless otherwise stated)

440

Sampling area in bakery	$\overline{A_{(combined)}}$	SD	SD as % on the average
Confectionary	9.1	3.9	43
Pastry	13.5	12.9	96
Weighing in area	78.6*	100.2*	127*

441 *n=4

442

443

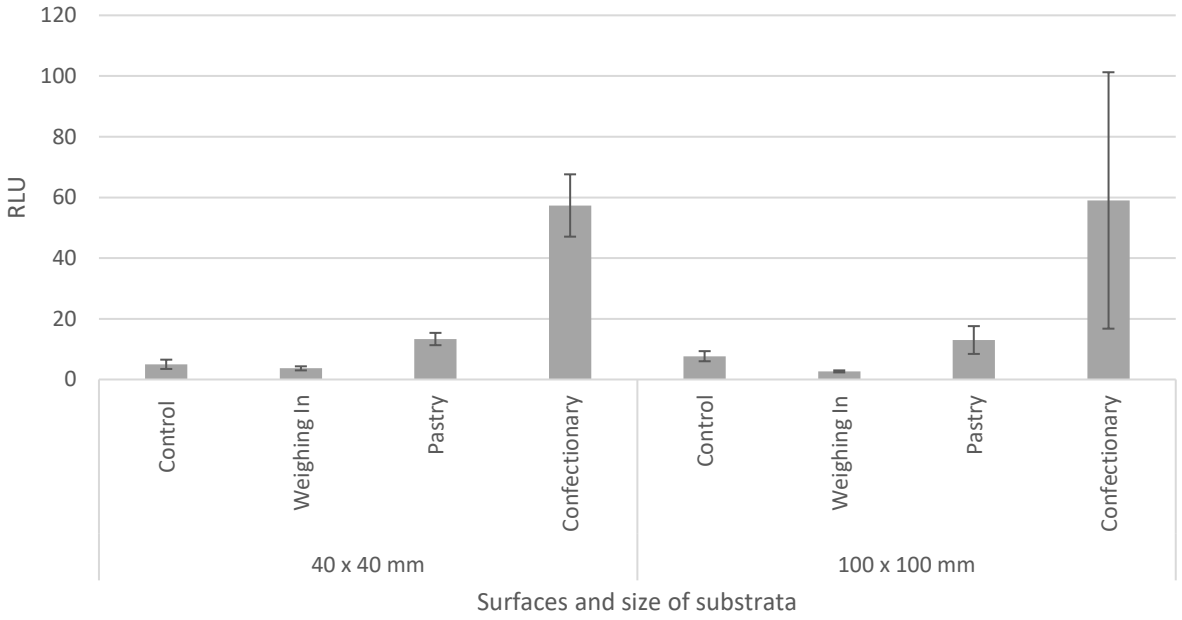

Figure 1. ATP bioluminescence measurements indicating microbial presence on the stainless steel surface of the three areas of the bakery using, (where routine cleaning pass mark = 30)

461

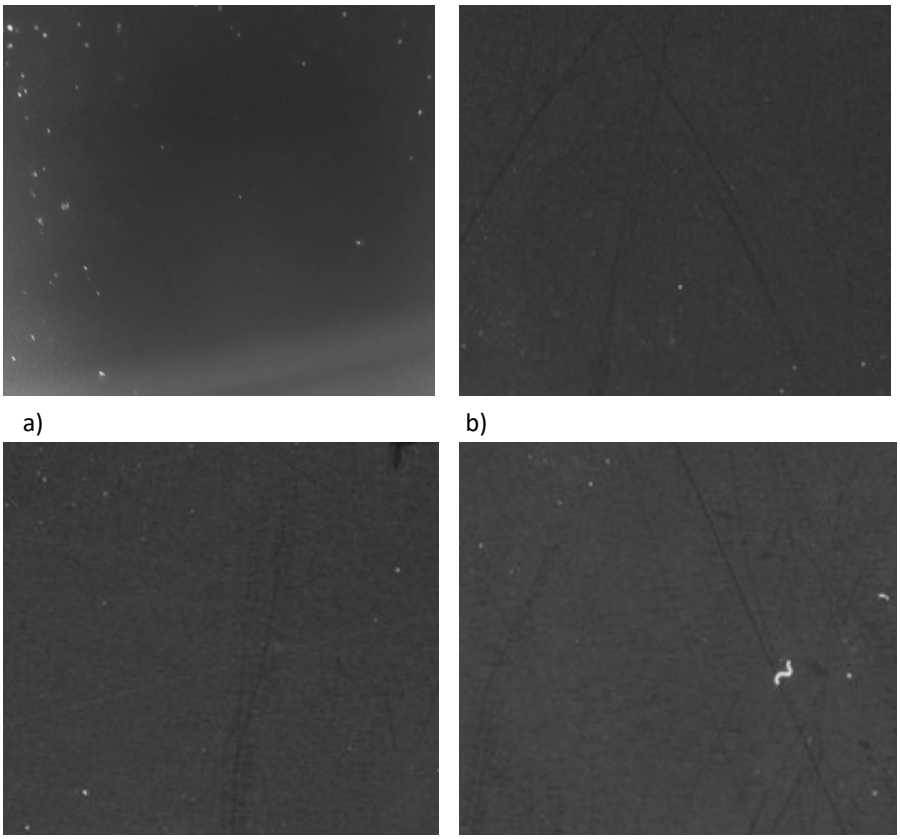

462

463 Figure 2. UV of stainless steel substrata obtained from the a) control surface b) weighing in area,

464 c) the pastry preparation area and d) the confectionary production area.

465

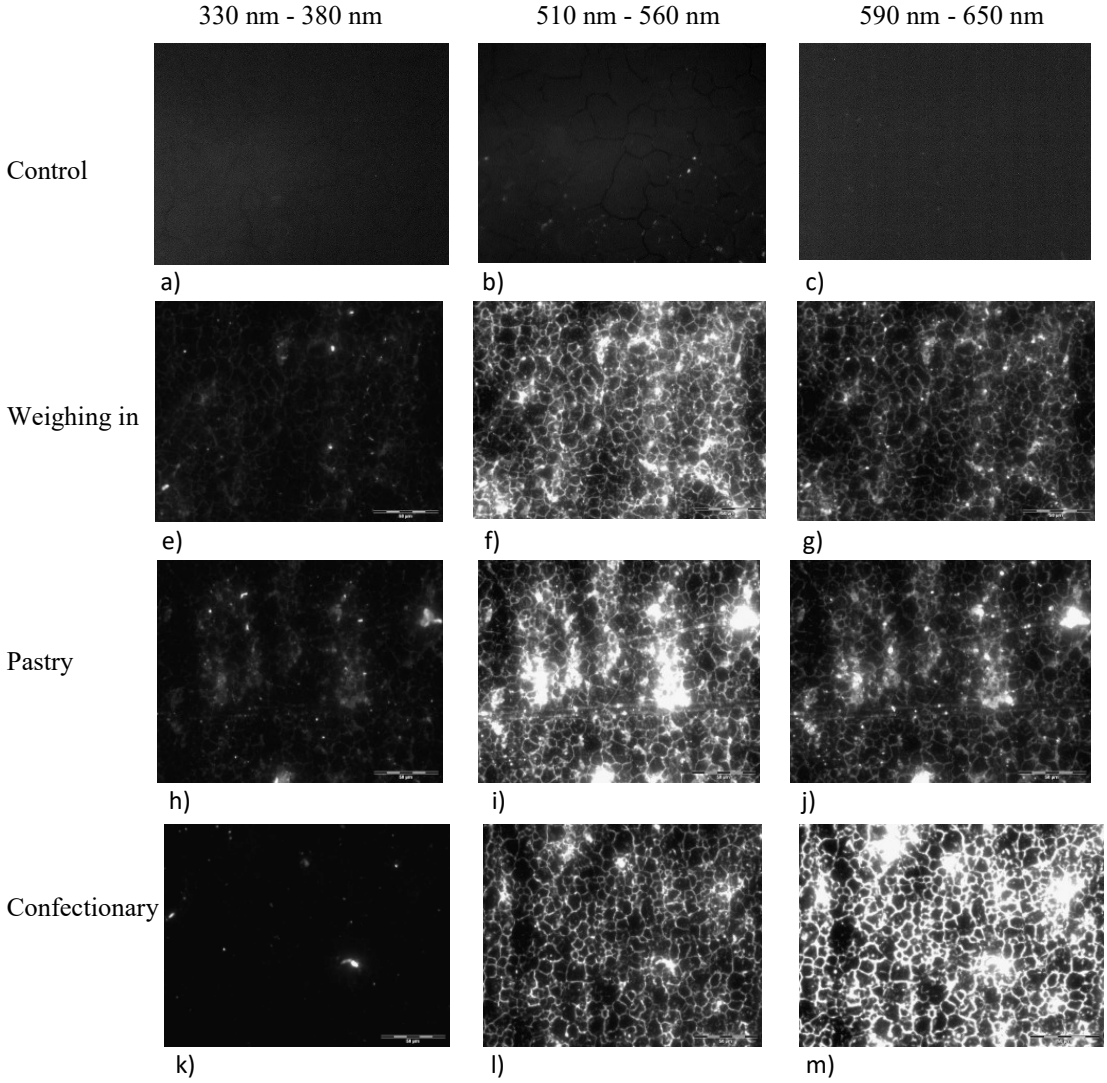

Figure 3. Organic matter coverage of stainless steel surfaces upon UV illumination from a) control, b) weighing in area, c) pastry area d) confectionary area of the bakery

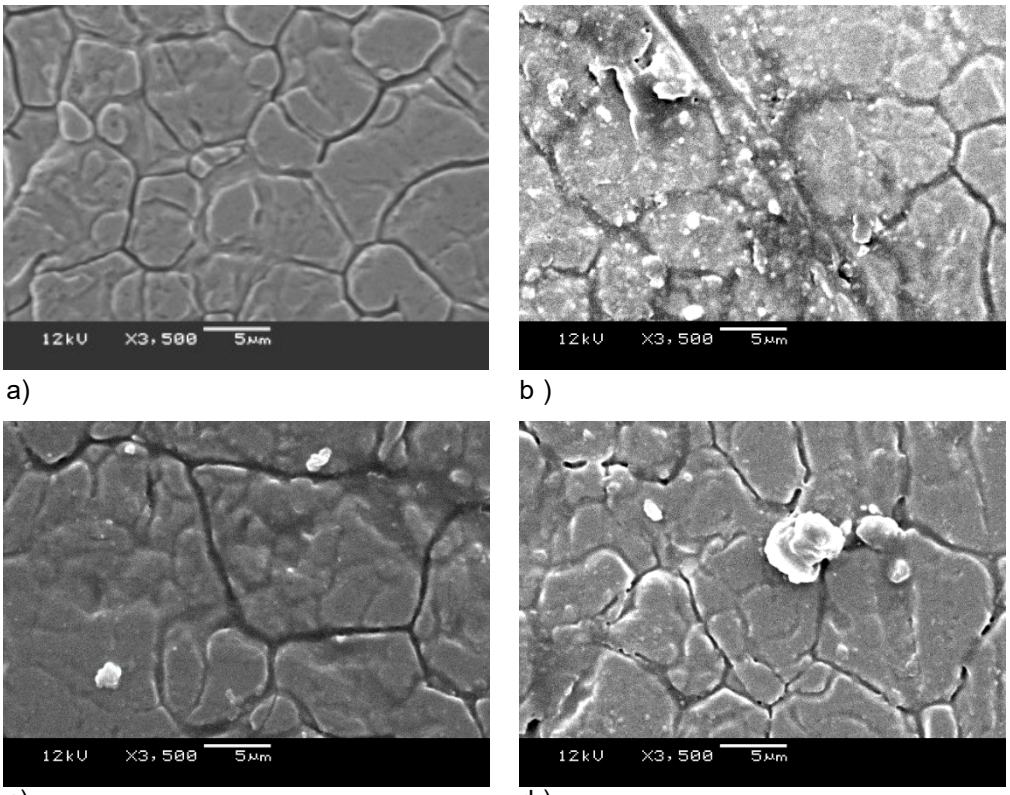

a) b)

c) d)

471

472 Figure 4. SEM images of stainless steel surfaces obtained from the bakery a) control, b), weighing

473 in area c, pastry area and d) confectionary area (x 3500 magnification)

474

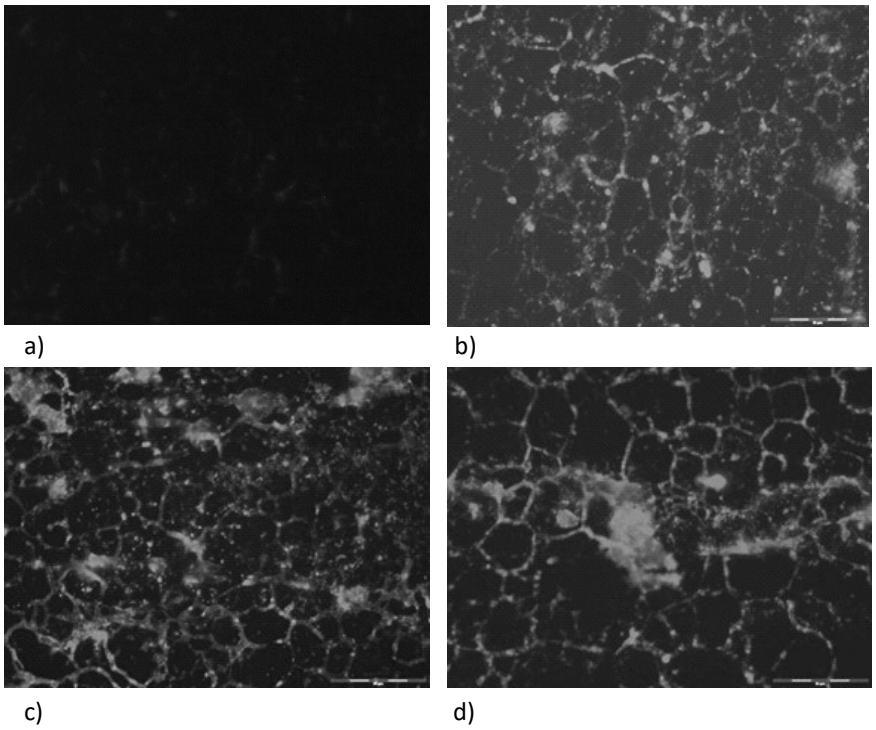

475

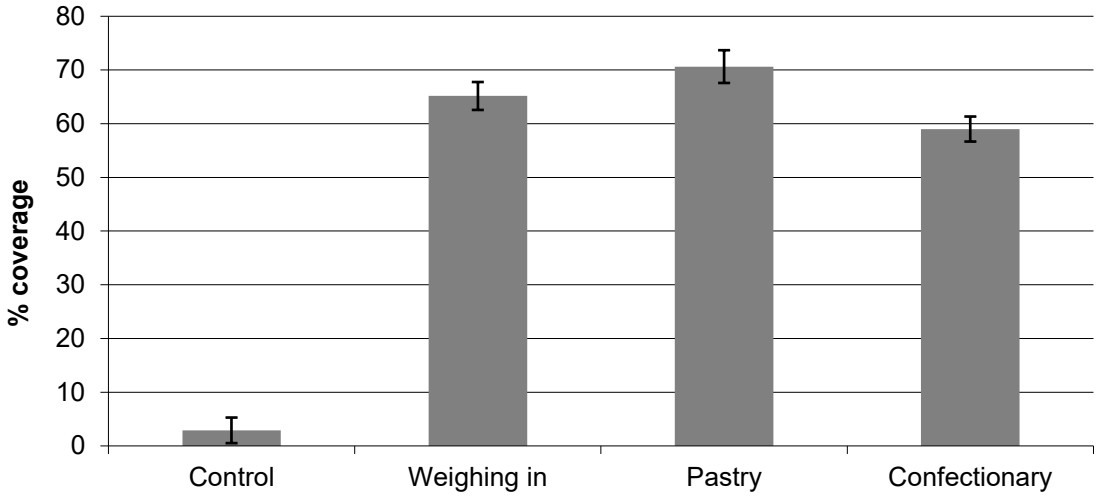

476

477 e)

478 Figure 5 Images showing organic matter coverage of stainless steel surfaces from a) control, b)
479 weighing in area, c) pastry area d) confectionary area of the bakery and e) percentage organic
480 material coverage of stainless steel surfaces sampled from the industrial bakery

481

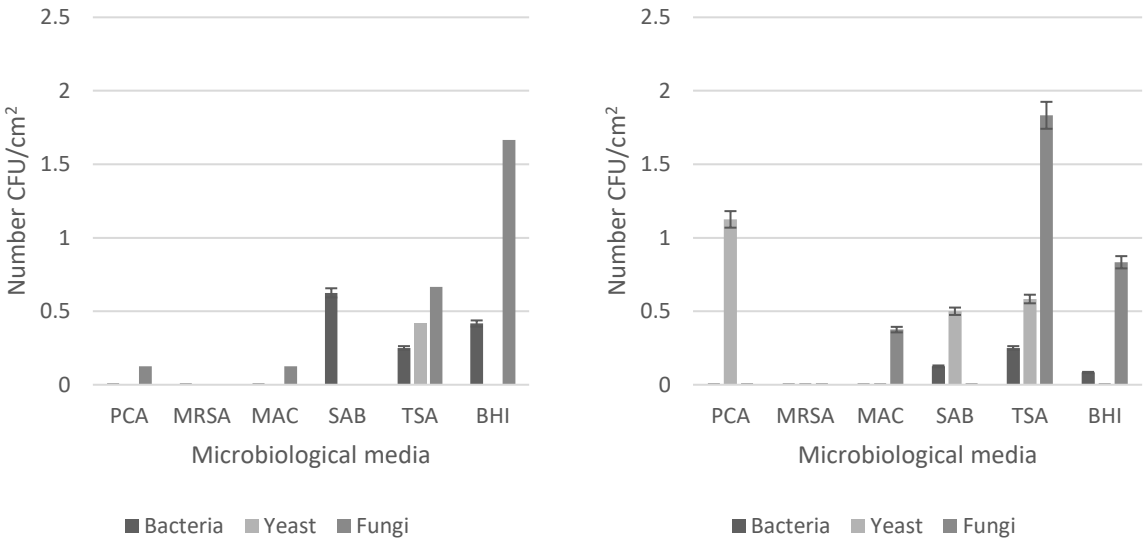

a) b)

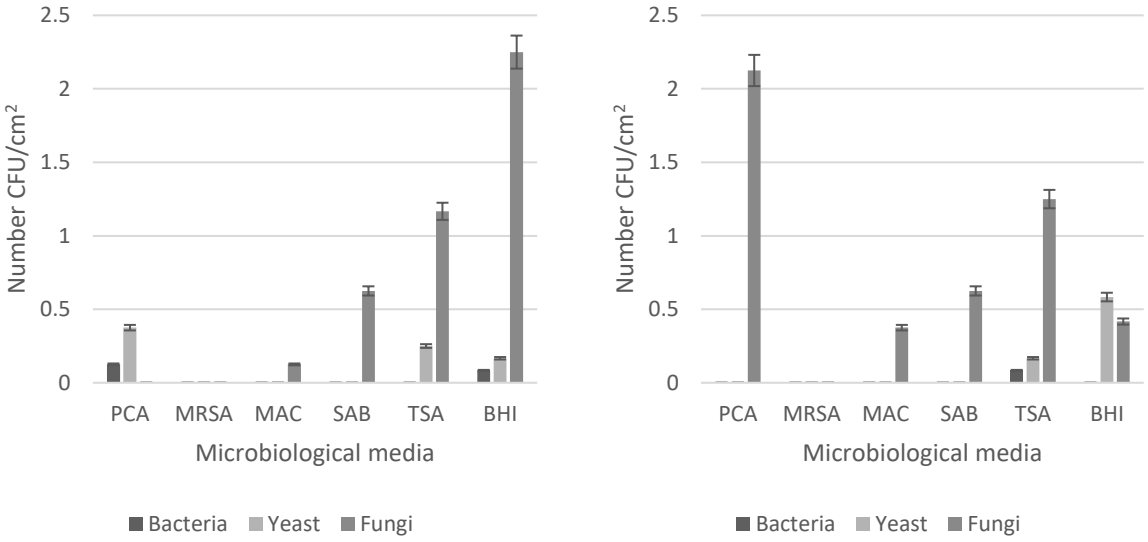

c) d)

Figure 6. The microbial count obtained from Stainless steel substratum using contact agar plates a) control b) weighing in area, c) pastry and d) confectionary areas PCA = Plate count agar, MRSA = de Man, Rogosa, Sharpe agar, MAC = MacConkey agar, SAB = Sabouraud agar, TSA = Tryptone soya agar and BHIA = Brain heart infusion agar.

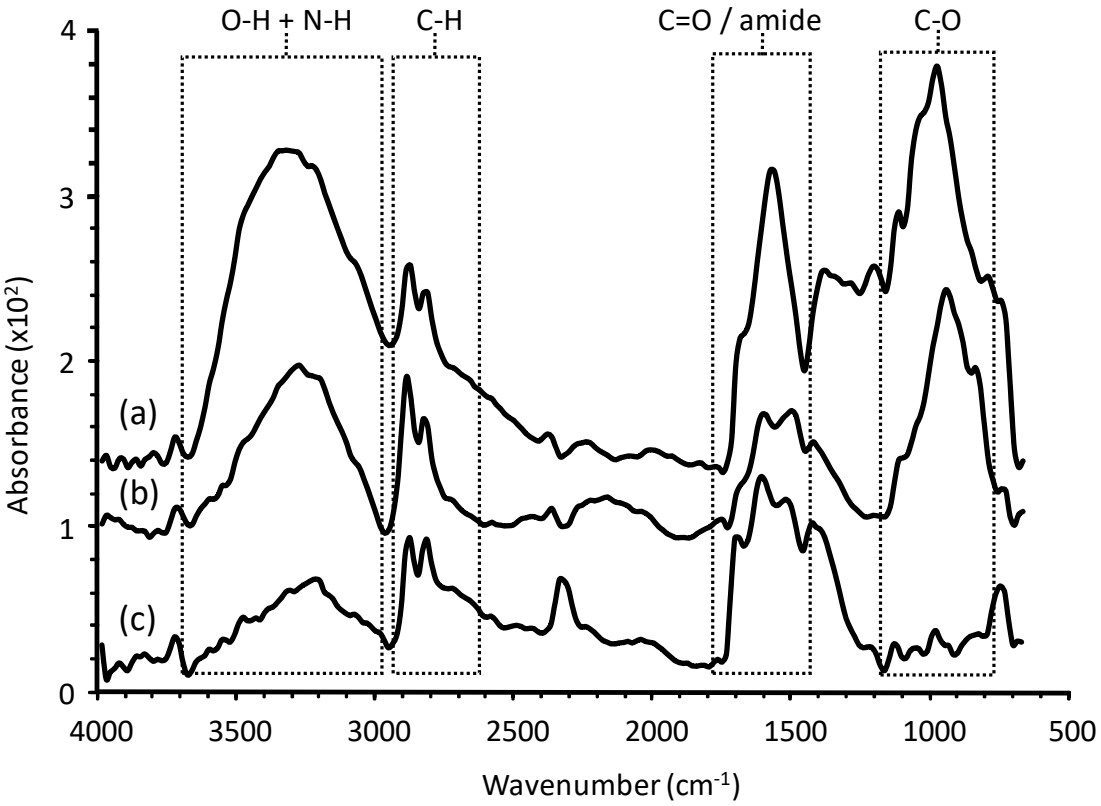

Figure 7. FTIR spectra of three representative samples taken from the a) weighing in area, b) confectionary and c) pastry areas. Note that the peak/baseline disturbance around 2340 cm^{-1} is due to atmospheric CO_2.